Global Journal of Engineering and Technology Advances
eISSN: 2582-5003
Cross Ref DOI: 10.30574/gjeta
Journal homepage: https://gjeta.com/

(RESEARCH ARTICLE)

Check for updates

Biosynthesis and characterization of (Co_3O_4) for solar cell applications via N-Sativa extract

Hameed Hussein Ahmed [1,*], Abduallah Mahmoud Ali [1] and Ahmed Naji Abed [2]

[1] *Department of Physics, College of Education for Pure Sciences, Tikrit University, Iraq.*
[2] *Department of Physics, College of Science, Mustansiriya University, Iraq.*

Global Journal of Engineering and Technology Advances, 2023, 14(03), 033–041

Publication history: Received on 24 January 2023; revised on 10 March 2023; accepted on 12 March 2023

Article DOI: https://doi.org/10.30574/gjeta.2023.14.3.0050

Abstract

Cobalt oxide (Co3O4) NPs was created utilizing *Nigella sativa* extract and the green synthesis process, and it was then dropped onto a glass substrate. The crystal structural makeup of Nano-particles was ascertained using the X-ray diffraction (XRD) pattern. and described as a material function for applications such as solar cells and light detectors. The surface morphology revealed the surface of (Co_3O_4)-coated municipal embroidery by inspecting the XRD, According to XRD measured data, all of the films are Nano-crystallized in the cubic spinel configuration and have an uniform dispersion seven main peaks correspond to the (2θ,hkl) 18.9544o-(111), 31.1402o-(220), 36.6685o-(311), 44.6107o-(400), 59.4292o-(332), 65.2836o-(440), 77.31370-(333). These improvements have an effect on the optical characteristics. The optical band gap was calculated using the absorption coefficient The optical band gap energy Eg1=2.2 eV, Eg1=3.7 eV was encountered by us. In contrast, In order to identify the functional groups present in bismuth oxide molecules, FTIR analysis revealed the strength of infrared absorption as a function of wavelength, as seen in the Co-O band. On the other hand, the FTIR analysis. Using FE-SEM morphology, the incorporation of nano-crystaline in various sizes and forms was examined. The prepared films' AFM pictures are displayed [Avg. Dimensions are 75.62 nm, 1.39 roughness units, and 1.68 nm root mean square .The optical and structural properties of Co3O4 nanoparticle films were investigated in order to determine the optical energy gap and crystallite size. revealed the presence of the tetragonal phase... Finally, the (I-V) and find the parameter of solar cell (Ag / Co3O4 / Psi /Si / Ag) are filling factor is FF= 29.62 and transformation Efficiency η =3.2%.

Keywords: *Nigella sativa*; Drop casting technique; Co_3O_4 thin film; Nano-particles; Solar cell

1. Introduction

Among the many metal oxides, transition metal structures and spinel structures have attracted more attention for their sensing capabilities in many fields such as catalysis, optoelectronic devices, magnetic data storage, biomaterials, electronics, bio/gas sensors, etc [1,2]. Cobalt oxide thin films are of interest to many researchers; Because it has desirable structural and optical properties, It has a different chemical formula (CoO, Co_2O_3, Co_3O_4), Co_3O_4 is the most stable of these oxides [3]. Cobalt oxide films are used in various applications, Cobalt oxide films are used in various applications, such as energy storage devices, gas sensors, solar cells, and some other applications on superconducting materials [4]. Nano-particles are synthesized in various ways within the framework of chemical, physical and biological processing [5]. These methods differ in terms of cost, particle size and distribution in terms of size and shape. The physical method has its drawbacks that make it less used, such as the high cost and it takes a longer period of time to produce [6]. The chemical synthesis method also has a high production capacity of Nano-particles, However, it is not without some drawbacks, as it requires strong reducing agents and is of high cost and toxicity [7]. As for the biosynthesis process, which is the subject of our study in this research, Which contributed to opening new horizons in the development of the production of nanomaterials at a lower cost and with low toxicity, which depend on oxidation and

* Corresponding author: Hameed Hussein Ahmed

reduction reactions [8]. The following is a table of properties of cobalt oxide, Cobalt oxide is an important p-type semiconductor with direct optical band gaps and an intense sub-gap absorption between (1.75 eV, 3.1 eV) [9].

Table 1 The properties of cobalt oxide (bulk) Co_3O_4

Chemical symbol	**Co3O4NPs**
Energy gap	1.75 – 3.1 eV
Transmission	565 nm444-
Color	brown
Density	6.11 g/cm3
Molar mass	74.93 g/mol
Group	Cobalt 9/ Oxygen 16
Electronic configuration	Cobalt [Ar] 3d7 4s2/ Oxygen [He] 2s2 2p4
Melting point	895 oC
Boiling point	900 oC

2. Materials and method

2.1. Thin films preparation and solar cell fabrication

The aqueous solution of the plant extract was prepared by crushing *Nigella sativa* seeds with an electric mixer, type (Crest-1) made in Germany. We obtained a soluble powder and then (1 g) of it was taken and placed in a heat-resistant flask. Then we added (100 ml) of distilled water. The powder is mixed with the added water by a magnetic stirrer at a temperature of (80 Co) for half an hour. Then we get the plant extract being filtered by filtration paper and display the ultrasound generation to observe the males and solids and avoid accumulation of solution. Green Synthesis method. 2.2 Cobalt oxide Preparing by using A cobalt nitrate solution was prepared at a concentration of (0.1 mol) and weighted (2.91gm) from ($Co(No_3).6H_2O$) (99.9%). Purity is a pale pink powder of the same molecular weight (182.47g/mol) and density (2.49g/cm3). Then it is dissolved in 200 ml of distilled water and the solution is mixed by a magnetic stirrer at (80 Co) with the addition of (5 ml) of (Hcl) acid for the purpose of accelerating the dissolution process. Then add (20 ml) of plant extract gradually through the dropper. After obtaining the aqueous solution of cobalt oxide, the resulting solution is bombarded by ultrasonic waves to break up the undissolved blocks and undissembled bonds and obtain a clear and homogeneous Nano-solution. Fig. 1-(a,b) shows the mechanism of synthesis of cobalt oxide.

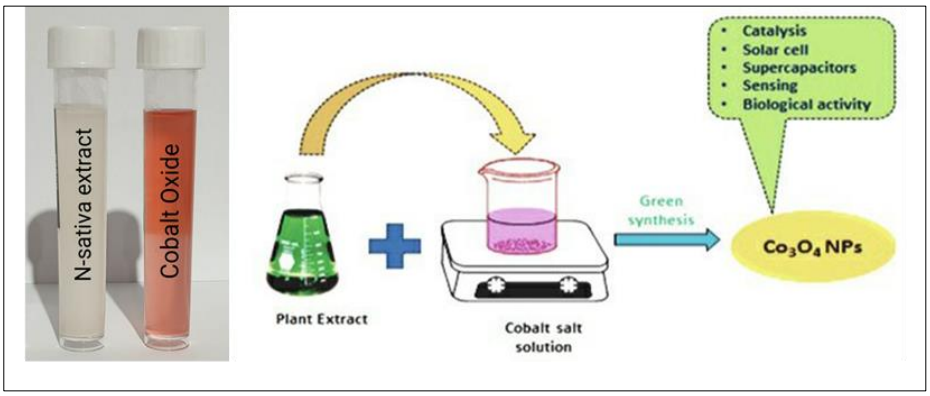

Figure 1 Cobalt oxide synthesis mechanism, b. prepared solutions

2.2. Synthesis thin film of Co3O4

Drop casting was implemented to deposit the nano-cobalt oxide solution as the glass/psi substrates were heated to a temperature of (70 ± 10 C°) In order to properly precipitate the prepared nano-cobalt oxide solution, for instance, we

placed three drops of the solution onto the glass slides on an electric heater fitted with a digital thermocouple and left it there for 30 minutes (XRD, UV-visible, FT-IR,SEM and TEM) By contrasting it with the international card JCPDS, it was possible to validate the material's identity and the presence of Nano-particles. The drop casting method of deposition is depicted in figure.

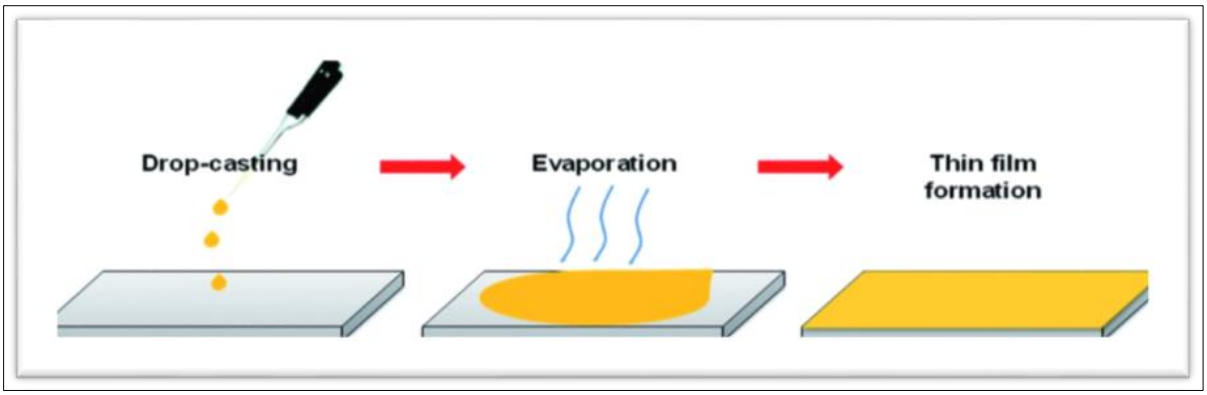

Figure 2 The drop casting process [10]

It is possible to better understand the method for creating cobalt oxide Nano-particles, crucial diagnostic tests, how to use them as solar cells, and how to measure their parameters.

3. Results and Discussions

3.1. X-ray diffraction

XRD the X-ray pattern showed the presence of nine distinct peaks, which correspond to the angles (18.95, 31.14, 36.66, 44.61, 59.42, 65.28, 77.31), As shown in Table 1.

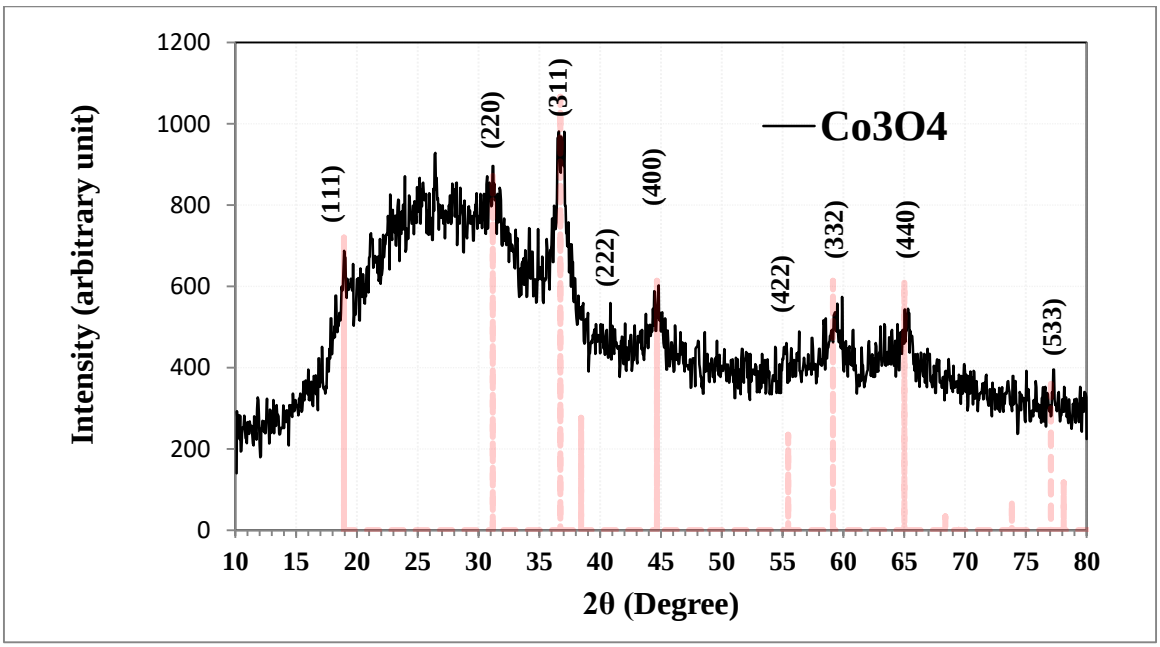

Figure 3 XRD pattern of Co_3O_4Nps film

X-ray diffraction was used to measure the structural characteristics, In order to examine the crystal structure, and to know the nature of crystal growth, and crystal plans of (pure: Co_3O_4) films deposited by drop casting method onto glass substrate. Through X-ray spectrum analysis for Co_3O_4 layer as in figure 1. The X-ray pattern shows the presence of several diffraction peaks for crystal levels, which shows that the crystal structure of the precipitated film is polycrystalline. XRD pattern agreement with values stander card No. 96-500-0225, this result acoording with [10].

Table 1 Result of inter planer for XRD

2θ (deg)	d_{hkl} (A°)	FWHM (deg)	G_S (nm)	phase	hkl	Card No.
18.9544	4.6783	0.4283	18.8	Co_3O_4	(111)	96-500-0225
31.1402	2.8698	0.7786	10.6	Co_3O_4	(220)	96-500-0225
36.6685	2.4488	0.6229	13.4	Co_3O_4	(311)	96-500-0225
44.6107	2.0295	0.7787	11.0	Co_3O_4	(400)	96-500-0225
59.4292	1.5583	0.7397	12.4	Co_3O_4	(332)	96-500-0225
65.2836	1.4281	0.7786	12.1	Co_3O_4	(440)	96-500-0225
77.3137	1.2332	0.5061	20.1	Co_3O_4	(333)	96-500-0225

3.2. AFM

Micrographs were used to determine the surface morphology of pure Co3O4 prepared by green synthesis and deposited using the drop casting method on a glass substrate at 60 = 20 C° at thicknesses of film was 260 nm.

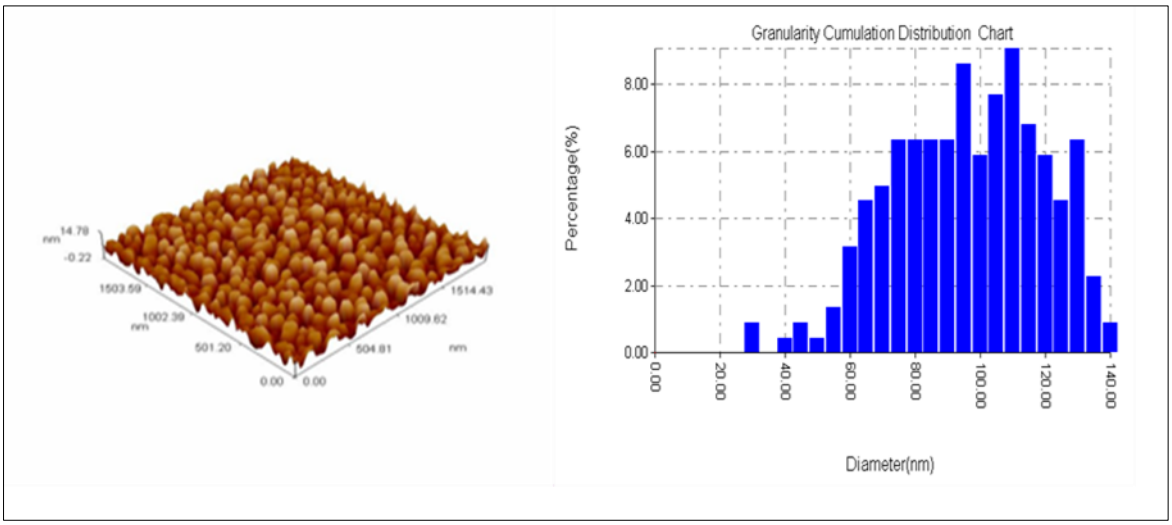

Figure 4 AFM image of the prepared films and granulanity cumulating distribution. Chart

Table 2 AFM data for undoped (Pure Co_3O_4)

Item	Avg. Diameter(nm)	Roughness average (nm)	(rms) (nm)
Pure Co3O4	75.62	1.39	1.68

3.3. FE-SEM

Field effect scanning electron microscope used to morphology of surface study, The findings demonstrated the thin films' high quality and demonstrated that they have a homogeneous surface shape over the entire substrate. Particles are smallest and distributed evenly over flat surfaces in the first image. The film was shown to be extremely dense an Co_3O_4 d have a uniform surface in this photograph. The nanocrystal clustered was seen in pure film.

The diameters of the Co_3O_4 particles ranged from 60 to 125 nm, as shown by the SEM images that the films have good surface coverage. EDS energy dispersive x-ray spectrograph, Which gives a map of the elements that make up the sample.

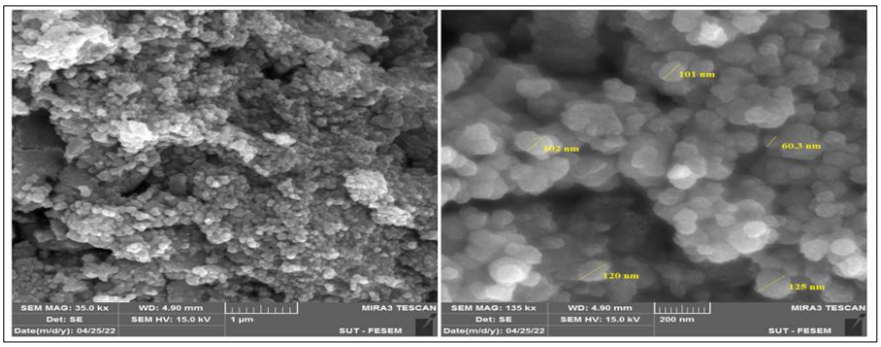

Figure 5 FE-SEM image for Co_3O_4 film

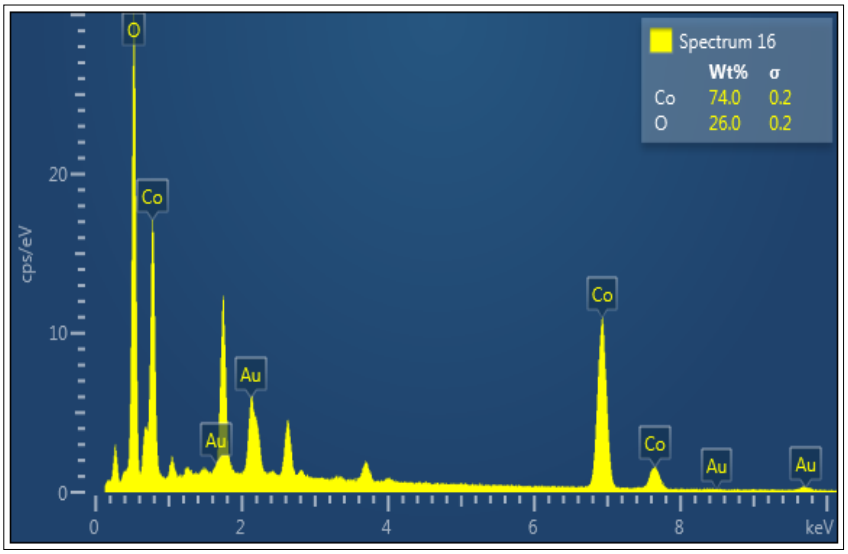

Figure 6 EDX for Co_3O_4 film

3.4. FT-IR

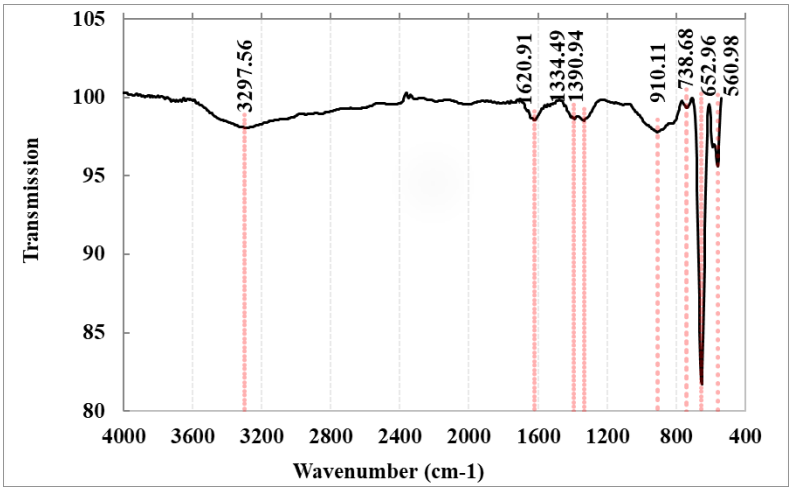

Figure 7 FTIR was measured for cobalt oxide thin film deposited on glass

Spectral measurements of the cobalt oxide film showed absorption bands as shown in Table 3, which shows the effective chemical bonds and their correspondence with the chemical composition. Results for the cobalt oxide thin film depicted in Figure 7. And Table 3 contains the bond structure. FT-IR analysis of the cobalt Co_3O_4 a sample surface was performed Where the sharp edge is centered at 1620.91cm^{-1}(O-H Scissors) ,1390.94cm^{-1}(C-H), And 3297.56cm^{-1} (O-H Stretch) on

the absorbent surface and represents a vibrating ring. While the top of peaks at 652.96cm^{-1}, 560.98cm^{-1} it represents the vibration of the linking between Co^{3+}-O and Co^{2+}-O and Oxygen element This is evidence of the existence of Co_3O_4 crystalline.

Table 3 FTIR Assessment for Co_3O_4

Band type	FT-IR of (Co)
O-H Stretch	3297.56
O-H Scissors	1620.91
C-H	1390.94
C-H	1334.49
C-O	1250.89
C-H	738.96
Co^{2+}-O	738.96
Co^{2+}-O	560.98

3.5. Optical Characteristics

It was established that cobalt oxide Nano-particles were present by looking at the ultraviolet spectrum (UV-VIS). Additionally, it was shown that absorption coefficient occurred at 27×10^4 cm^{-1} at λ=292 nm (IR-region) and 17×10^4 cm^{-1} at λ=520 nm (VIS-region) when scanning between wavelengths of 300 to 900 nm. And in the photon energy range of 1 to 7 eV, the optical energy gaps of Co3o4 NPs are Eg_1= 2.4 eV and Eg_2= 3.7 eV. This is obtained by plotting the magnitude $(\alpha h\upsilon)^2$ as a function of photon energy (hυ), as seen in figure 8. As the material transforms into a nano state, the energy gap widens again to that point

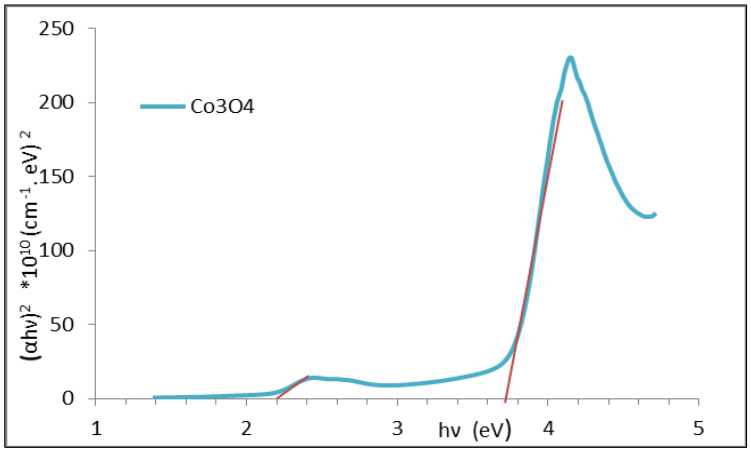

Figure 8 Plot of $(\alpha h\upsilon)^2$ versus (hυ) of Co_3O_4 NPs thin film

The optical absorption coefficient (α) was calculated from the absorbance spectrum of the prepared films, using the (1) relationship, as it was found that all films have an absorption coefficient greater than (1×10^4cm^{-1}) in the visible spectrum, and this means that the films have an optical energy gap Directly, as well as through experimental calculations, it was found that the value of (r) in equation (2) is equal to (1/2) for the film. The emergence of more than one energy gap is evidence of the fission of electronic levels and the generation of local levels within the prohibited energy gap according confinement phenomena.

$$\alpha=2.303\ \frac{A}{t} \quad \ldots\ldots\ldots\ldots\ldots\ldots\ldots\ldots\ (1)$$

$$\alpha h\upsilon= \ldots\ldots\ldots\ldots\ldots\ldots\ldots(2)$$

$$\alpha h\upsilon = A_o\left(h\upsilon\text{-}E_g\right)^r \text{ ……..(2)}$$

3.6. Electrical characterization

A solar cell is a device that efficiently transforms light energy into electrical energy. Figures 9a,b and 9b exhibit the (I-V) in the dark and the (I-V) illuminated both of a solar cell's most significant electrical characteristics.

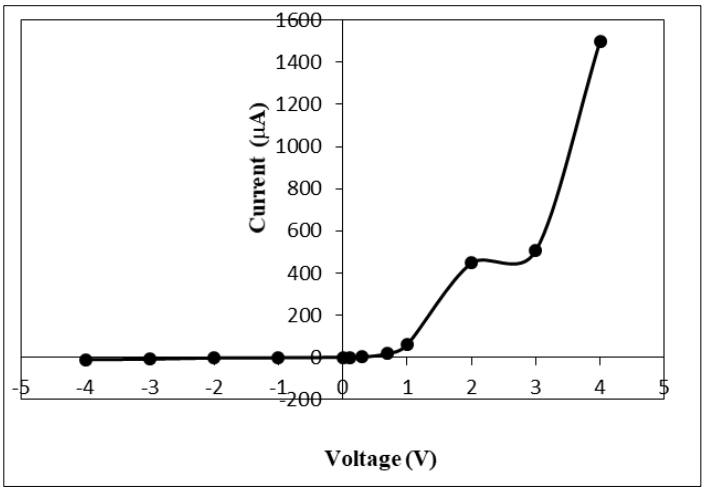

Figure 9 a-(I-V) characteristics of (Ag/ Co_3O_4/PSi//Si/Ag) in dark

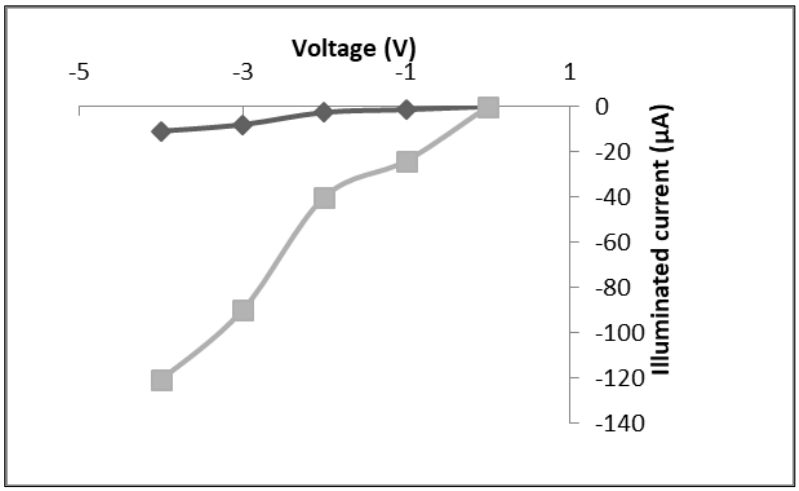

Figure 9 b-(I-V) characteristics of (Ag/ Co_3O_4/PSi//Si/Ag) in illuminated

The characteristics of the current-voltage are important to determine the real performance of solar cells by calculating the values of a number of parameters After projecting the processed light rays from a light source perpendicular (θ=0) to a certain intensity on the cell, By gradually changing the value of the load resistance (R_L) in the range (0-∞), it was possible to measure the current-voltage characteristics using digital ammeters and voltmeters, and to ensure the stability of the temperature and intensity of illumination on the solar cell during the period of making measurements (measurement of current and voltage for each value of resistance), as a value (Voc) was measured at (R_L= ∞) The value of I_{SC} at (R_L=0), And then a (FF=32) calculation from Equation (3) in order to calculate the efficiency ($\eta\% = 3$) of the solar cell from Equation (4).

$$F.F = \frac{I_m.V_m}{I_{SC}.V_{OC}} \text{ ……..(1)}$$

$$\eta = \frac{I_{SC}.(V_{OC}).F.F}{P_{in}} \text{ ……..(2)}$$

FF: filling factor, η: efficiency of solarcell, I_m: maximum current density, V_m: maximum voltage, I_{sc}: short circuit current, V_{oc}: open circuit voltage, P_{in}: incident radiation power represent the amount of energy faling perpendiculary on unit area per unit time.

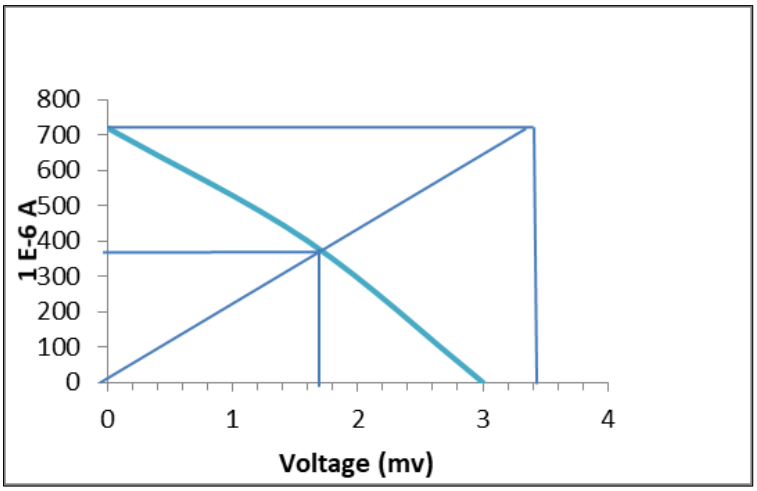

Figure 10 Characteristics of solar cell (Ag/ Co3O4/PSi//Si/Ag)

Table 3 Parameter of solarcell (Ag/ Co3O4/PSi//Si/Ag)

Voc(mV)	Isc(μA)	Vm(mV)	Im(μA)	R (mw/cm²)	F.F	Eff%
3	720	1.6	400	100	29.6	3.2

4. Conclusion

The precipitated cobalt oxide Co_3O_4 films were synthesis by drop casting method on glass substrates, Through optical examinations using the ultraviolet and visible spectrum, by Taus equation, the type of transmission (direct transmission) was identified with the presence of two optical energy gaps (Eg1=2.4eV,Eg2=3.7eV), one of it was located in the visible region (λ=517nm) and the other in the ultraviolet region (335nm), The green synthesis of Nano-particles gave good results, and this was proven by diagnostic tests. The solar (Ag/Co_3O_4/PSi/Si/Ag) cell had acceptable conversion efficiency, so the green synthesis method is a safe and promising method for future energy applications.

Compliance with ethical standards

Acknowledgments

Thanks and gratitude to the professors of the Department of Physics at the College of Education for Pure Sciences at the University of Tikrit, and I do not forget to extend my sincere thanks to the Department of Physics at the College of Science, Al-Mustansiriya University, for facilitating work in their scientific laboratories to accomplish this research.

Disclosure of conflict of interest

There is no conflict of interest.

References

[1] Hartono , A .; Sanjaya , E .; Ramli , R.(2018) Glucose Sensing Using Capacitive Biosensor Based on Polyvinylidene Fluoride Thin Film . Biosensors, 30 ; 8 (1) : 12.

[2] Marie , M .; Mandal , S .; Manasreh , O. (2015) An Electrochemical Glucose Sensor Based on Zinc Oxide Nanorods . Sensors 2015 , 15 , 18714-18723 ,

[3] Wang, L., Song, X. C., & Zheng, Y. F. (2012). Electrochromic properties of nonporous Co3O4 thin films prepared by electrodeposition method. Micro & Nano Letters, 7(10), 1026-1029.

[4] Tyagi, A., Banerjee, S., Cherusseri, J., & Kar, K. K. (2020). Characteristics of transition metal oxides. In Handbook of Nanocomposite Supercapacitor Materials I (pp. 91-123). Springer, Cham.

[5] Rane, A. V., Kanny, K., Abitha, V. K., & Thomas, S. (2018). Methods for synthesis of Nano-particles and fabrication of nanocomposites. In Synthesis of inorganic nanomaterials (pp. 121-139). Woodhead publishing,

[6] Salavati-Niasari, M., Mir, N., & Davar, F. (2009). Synthesis and characterization of Co3O4 Nano rods by thermal decomposition of cobalt oxalate. Journal of Physics and Chemistry of Solids, 70(5), 847-852.

[7] Natsuki, J., Natsuki, T., & Hashimoto, Y. (2015). A review of silver Nano-particles: synthesis methods, properties and applications. Int. J. Mater. Sci. Appl, 4(5), 325-332.

[8] Das, S., Chakraborty, J., Chatterjee, S., & Kumar, H. (2018). Prospects of biosynthesized nanomaterials for the remediation of organic and inorganic environmental contaminants. Environmental Science: Nano, 5(12), 2784-2808.

[9] Abdullah, M. M., Akhtar, M. S., & Al-Abbas, S. M. (2018). Facile growth and promising applications of cobalt oxide (Co3O4) Nano-particles as chemi-sensor and dielectric material. *Current Nanoscience*, *14*(4), 343-351.

[10] Smith, W. L., & Hobson, A. D. (1973). The structure of cobalt oxide, Co3O4. Acta Crystallographica Section B: Structural Crystallography and Crystal Chemistry, 29(2), 362-363